β-Cyclodextrin-Functionalized Fe₃O₄-Supported Pd-Nanocatalyst for the Reduction of Nitroarenes in Water at Mild Conditions

Kamrul Hasan,* Ihsan A. Shehadi, Reshma G. Joseph, Shashikant P. Patole, and Abdelaziz Elgamouz

Cite This: *ACS Omega* 2023, 8, 23901−23912

Read Online

ACCESS | Metrics & More | Article Recommendations | Supporting Information

ABSTRACT: In this study, a novel heterogeneous catalyst (Fe₃O₄@β-CD@Pd) has been developed by the deposition of palladium nanoparticles on the β-cyclodextrin-functionalized surface of magnetic Fe₃O₄. The catalyst was prepared by a simple chemical co-precipitation method and characterized extensively by using Fourier transform infrared (FTIR) spectroscopy, thermogravimetric analysis (TGA), X-ray diffraction (XRD), field-emission scanning electron microscopy (FE-SEM), energy dispersive X-ray spectroscopy (EDX), transmission electron microscopy (TEM), X-ray photoelectron spectroscopy (XPS), and inductively coupled plasma-optical emission spectrometry (ICP-OES) analyses. Herein, the applicability of the prepared material was evaluated for the catalytic reduction of environmentally toxic nitroarenes to the corresponding anilines. The catalyst Fe₃O₄@β-CD@Pd showed excellent efficiency for the reduction of nitroarenes in water under mild conditions. A low catalyst loading of 0.3 mol % Pd is found to be efficient for reducing nitroarenes in excellent to good (99−95%) yields along with high TON values (up to 330). Nevertheless, the catalyst was recycled and reused up to the 5th cycle of reduction of nitroarene without any loss of significant catalytic activity.
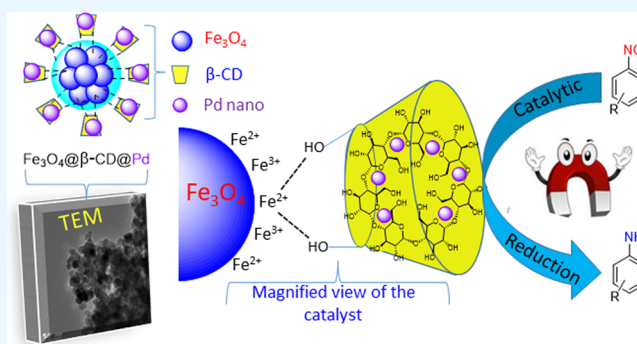
1. INTRODUCTION

Designing new heterogeneous catalytic processes which are environmentally friendly is still an ultimate goal for many critical industrial processes and pharmaceutical applications.[1−4] One approach to achieve the green socio-economic benefits is to design new catalysts that are supported on bio-polymers, supramolecules, and other scaffolding materials. The excellent capabilities of these materials lie in improving the recyclability, the selectivity, and the activity of catalysts as well as the rate of the chemical reactions and high conversions and product selectivity.[5−7] In the past few years, cyclodextrins have been widely used as a support in catalytic synthesis of bi-aryl and aryl-olefinic compounds through Suzuki−Miyaura C−C which produces a wide range of natural and medicinal compounds. Palladium-based catalysts are of special interest to medicinal and pharmaceutical industries due to the possibility of producing a wide range of potential derivatives with biological activities.[8−10]

Using β-cyclodextrin (β-CD)-supported catalysts has been reported for many heterogeneous catalysts as palladium, copper, iron, other metals, and mixed metal oxides.[3,11] β-CDs are relatively cheap, biodegradable, nontoxic, abundant, and easily tunable supramolecule oligosaccharides with hydrophobic cone-shaped cavity and hydrophilic surface due to the abundance of hydroxyl groups in the α-1,4 linked D-glucopyranose units.[12] Therefore, cyclodextrins are excellent drug carriers that are widely used in the formulation processes

of the pharmaceutical industries. In addition to being water soluble, cyclodextrins can be also easily functionalized and modified which enable enormous benefit and opportunities including selective solubility in a desired solvent and application in catalysis.[13] Due to its hydrophobic nature, the cavity in β-CD can encapsulate small organic molecules, and inclusion complexes are formed. Such formation of host-guest molecules are deemed important in catalytic removal of pollutants from air and water.[14]

Nitro-compounds are one of the major toxic pollutants that are needed to be dealt with as they are being produced by pesticides, dyes, and textile industries.[15] Nitroarenes and other aromatic nitro compounds are a commonly occurring pollutant in industrial waste. Their presence in the environment can have severe negative impacts due to their nonbiodegradable and carcinogenic nature.[16] The United States Environmental Protection Agency (US-EPA) has classified nitroarenes as priority pollutants under the clean water act because of the dangers they pose and suggests maintaining their concen-
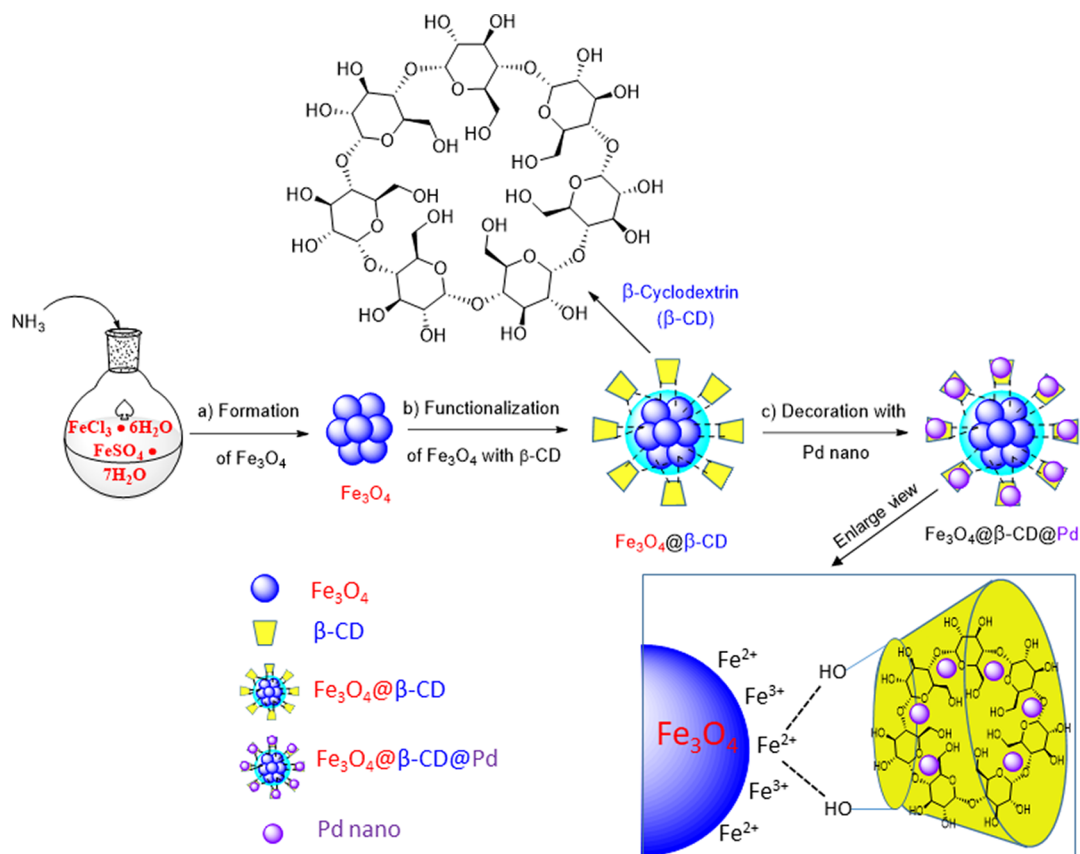
Scheme 1. Detailed Synthetic Procedure of the β-CD-Functionalized Fe$_3$O$_4$-Based Pd Nanocatalyst (Fe$_3$O$_4$@ β-CD@Pd) Following the Reaction Conditions: (a) H$_2$O, NH$_3$, 90 °C, N$_2$ (b) H$_2$O, β-CD RT (c) EtOH, Pd(OAc)$_2$, NaBH$_4$, RT.

tration (as low as 10.0 ng/mL) in natural water bodies.[17] Therefore, reducing nitroarenes to less or nontoxic amines and other nontoxic forms of compounds is considered an important strategy for pollution prevention and clean up. One of the most studies nitroarene derivatives in both academia and industrial research is the reduction of 4-nitrophenol (4-NP) to 4-aminophenol (4-AP). Noble transition-metal-based nanoparticles such as Pd, Au, and Ag are the active ingredients of the catalysts while impregnated with solid support such as Fe$_3$O$_4$, r-GO, and kaolin which play a significant role in the catalytic reduction of 4-NP.[18−24] Recent literature survey also shows that using a cross-linked Pd/β-CD system is a proven catalytic process for the reduction of nitroarenes and related azo-dyes to amines.[10,25−27]

Moreover, in recent years, using magnetically responsive materials like Fe$_3$O$_4$ (MNs)-core which are supported on nano-structured transition metal heterogeneous catalysts is gaining a lot of attention as they are environmentally friendly and exhibit easiness of the recyclability of the catalysts.[10,26] Such systems provide dynamic flexibility through which the contact between the catalyst and reactants is enhanced, hence increasing immensely the activity of the catalysts.[20,28] These special features of Fe$_3$O$_4$ encouraged us to pursue the development of green and sustainable Fe$_3$O$_4$-based heterogeneous catalysts. Recently, our research group and by others have explored Fe$_3$O$_4$-based heterogeneous catalysts for important organic transformations, including chemoselective *N*-arylation of *O*-alkyl primary carbamates,[29,30] domino synthesis of carbamates and unsymmetrical urea,[31,32] nitro-arene reduction,[33] C−C cross-coupling,[34,35] oxidative amina-

tion,[36] A^3 coupling,[37] and ester synthesis.[38] In the continuation of our efforts, herein, we have synthesized and characterized for the first time a β-cyclodextrin-functionalized Fe$_3$O$_4$-supported Pd-nanocatalyst for the reduction of the toxic nitro-arenes to the corresponding aniline derivatives.

Details synthesis of the catalyst is shown in Scheme 1. The progress and identification of the products of the catalytic reduction of nitroarenes are monitored by GC−MS.

2. MATERIALS AND METHODS

2.1. Chemicals and Reagents. All chemical reagents including iron(III) chloride hexahydrate (FeCl$_3$·6H$_2$O; 98%), Fe(II) sulfate heptahydrate (FeSO$_4$·7H$_2$O; 99%), ammonium hydroxide (NH$_4$OH; 30−33%), ethanol (EtOH; 96%), β-cyclodextrin (β-CD; C$_{42}$H$_{70}$O$_{35}$; 97%), palladium(II) acetate (Pd(OAC)$_2$; 99%), sodium borohydride (NaBH$_4$; 98%), and substituted nitroarenes were purchased from Aldrich. All chemicals were of analytical grade and used without any further purification. Ultrapure water was produced using a Milli-Q Elix Essential 5 water purification system and used in all experiments.

2.2. Synthesis of Fe$_3$O$_4$. Magnetic Fe$_3$O$_4$ was prepared by mixing FeCl$_3$·6H$_2$O and FeSO$_4$·7H$_2$O in water under nitrogen following the traditional co-precipitation method based on the adopted literature procedure.[39] Detailed synthesis of Fe$_3$O$_4$ has been discussed in the electronic Supporting Information (ESI).

2.3. Functionalization of Fe$_3$O$_4$ with β-CD (Fe$_3$O$_4$@β-CD). β-CD (1.0 g) was added to 75.0 mL of water and stirred for 1.0 h until all β-CD dissolved completely. Fe$_3$O$_4$ (1.0 g) was added to the aqueous solution of β-CD, and then, the
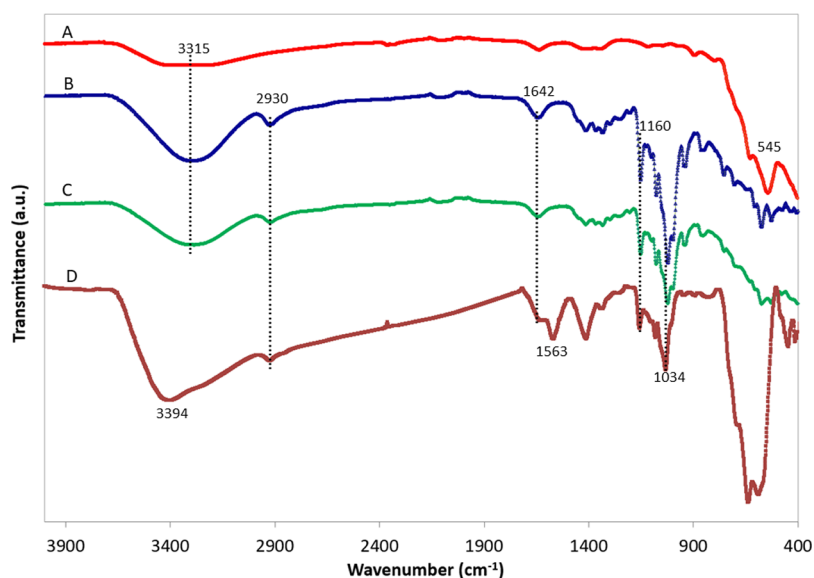
Figure 1. FTIR spectra of Fe_3O_4 (A), pure β-CD (B), $Fe_3O_4@\beta$-CD (C), and $Fe_3O_4@\beta$-CD@Pd (D).
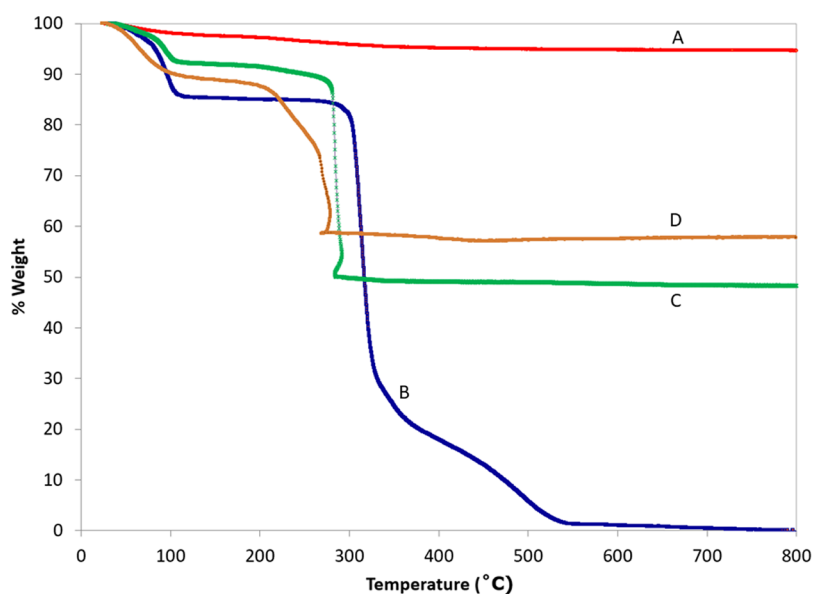
Figure 2. TGA curves for Fe_3O_4 (A), pure β-CD (B), $Fe_3O_4@\beta$-CD (C), and $Fe_3O_4@\beta$-CD@Pd (D).

mixture was stirred for another 4.0 h under room temperature (RT) of 22 °C. After successful functionalization of Fe_3O_4 with β-CD, the product $Fe_3O_4@\beta$-CD was separated with external magnet and washed with ethanol and dried at 60 °C for use in the next step.

2.4. Fabrication of the Catalyst $Fe_3O_4@\beta$-CD@Pd

$Fe_3O_4@\beta$-CD (1.0 g) was sonicated in 20.0 mL of ethanol for 30 min; then, 2.25 mmol (0.50 g) of $Pd(OAc)_2$ (dissolved in 15.0 mL of ethanol) was added to the suspension of $Fe_3O_4@\beta$-CD and stirred at RT for 2 h. $NaBH_4$ solution (2.5 mL of 0.25 M) was added dropwise with continuous stirring for a period of 4 h. The product, $Fe_3O_4@\beta$-CD@Pd, obtained as black solid materials was collected through separation with an external magnet, washed with ethanol (3 × 10.0 mL) to remove unreacted materials. The final product was dried in open air and stored for further application in nitroarenes reduction. Overall, synthetic procedure of the catalyst is presented in Scheme 1.

2.4. General Procedure for the Reduction of Nitro-arenes. Ultrapure water (3.0 mL) containing 1.0 mmol of the nitroarene substrate and 3.0 mg of the catalyst was stirred for a period of 5.0 min at RT. Subsequently, 2.0 mmol of $NaBH_4$ as the reductant was added to the above mixture. The reaction mixture was then stirred at 50 °C for an hour. The progression of the reduction reaction was monitored by thin layer chromatography (TLC) using hexane/ethyl acetate (3:1) as the eluent. After completion of the reaction, the catalyst $Fe_3O_4@\beta$-CD@Pd was separated with an external magnet. The reaction mixture was then extracted with ethyl acetate (3 × 10.0 mL) from the aqueous solution using a separatory funnel. The combined organic phases were dried with anhydrous Na_2SO_4, and finally, ethyl acetate was evaporated to obtain the desired product. The product formation and yield were determined by GC−MS.
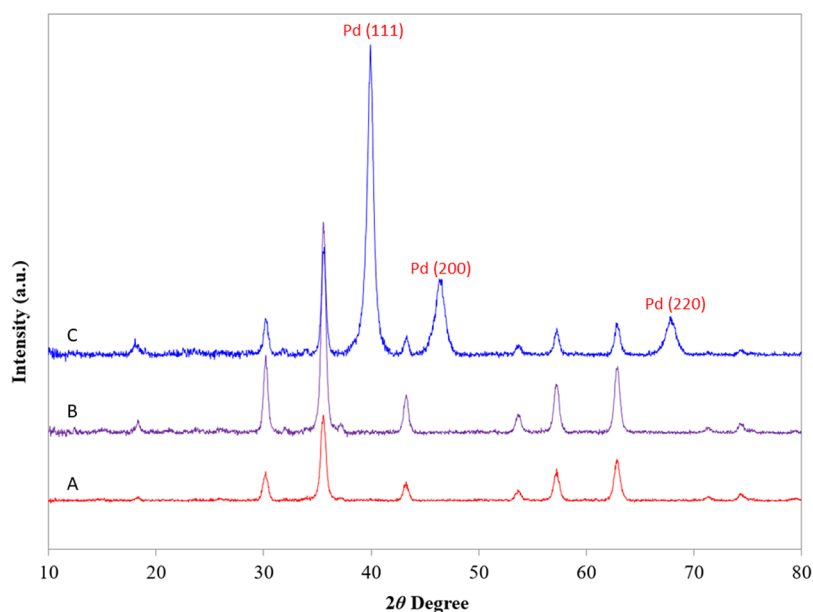
Figure 3. XRD pattern of bare Fe_3O_4 (A), $Fe_3O_4@\beta$-CD (B), and the catalyst $Fe_3O_4@\beta$-CD@Pd (C).

3. RESULT AND DISCUSSION

3.1. Characterization of the Catalyst $Fe_3O_4@\beta$-CD@Pd. The sequential functionalization of Fe_3O_4 with β-CD, followed by the deposition Pd nanoparticles, is established by FTIR spectra. For evidence, FTIR spectra of bare Fe_3O_4 (A), pure β-CD (B), β-CD functionalized MNs $Fe_3O_4@\beta$-CD (C), and β-cyclodextrin functionalized Fe_3O_4-supported Pd nanoparticles $Fe_3O_4@\beta$-CD@Pd (D) are shown in Figure 1. The FTIR spectrum of Fe_3O_4 exhibits the characteristic band attributed to the stretching vibration of Fe−O at 545 cm^{-1}, and the band at 3315 cm^{-1} is attributed to the O−H stretching vibration of adsorbed water on the surface of Fe_3O_4 (curve A). In the pure β-CD spectrum, appearance of strong bands at 3315, 2930, and 1642 cm^{-1} is attributed to the O−H stretching vibration, asymmetric C−H stretching vibration, and the C−O stretching vibration, respectively (curve B).[13,40,41]

Other two characteristics bands of pure β-CD are observed at 1160 and 1034 cm^{-1} which can be ascribed for the symmetric and antisymmetric glycoside C−O−C vibration of ether linkage in the β-CD ring.[13,40,41] The presence of all of these abovementioned bands in $Fe_3O_4@\beta$-CD (curve C) confirms the successful functionalization of Fe_3O_4 with β-CD. In the FTIR spectrum of $Fe_3O_4@\beta$-CD@Pd (curve D), the appearance of characteristics bands at 2930, 1160, 1034, and 583 cm^{-1} clearly confirms the presence of β-CD and Fe_3O_4 in the catalyst material. Also, a noticeable band shift in the FTIR spectrum of $Fe_3O_4@\beta$-CD@Pd from 3315 to 3394 cm^{-1} and 1642 to 1563 cm^{-1} reveals the effective decoration of β-CD with Pd nanoparticles, which is comparable with the literature-reported results.[14,42]

Thermal stability and nature of the component of the β-cyclodextrin functionalized Fe_3O_4-supported Pd nanoparticles $Fe_3O_4@\beta$-CD@Pd is estimated by the TGA with an evaluated weight % as the function of temperature. Figure 2 represents the TGA curves of bare Fe_3O_4 (A), pure β-CD (B), β-CD functionalized MNs $Fe_3O_4@\beta$-CD (C), and β-cyclodextrin functionalized Fe_3O_4-supported Pd nanoparticles $Fe_3O_4@\beta$-CD@Pd (D). The TGA analysis of bare Fe_3O_4 (Figure 2A)

indicates that there is only a 4% weight loss in the temperature range of 30 to 800 °C, which may be attributed to the loss of moisture content in the Fe_3O_4 sample. On the other hand, all other TGA curves (Figure 2B−D), except for Fe_3O_4, demonstrate a pseudo two-stage decomposition pattern as the temperature increases. The initial stage of thermal decomposition within 30−100 °C is associated with the removal of moisture or remaining solvent content from the nanocomposites. The subsequent stage involves the primary mass loss, which entails mainly the removal of organic moieties from the β-CD component. The TGA analysis clearly demonstrates that Fe_3O_4 has been functionalized with β-CD, as evidenced by the lower weight loss compared to pure β-CD (Figure 2B, C). Furthermore, the deposition of Pd nanoparticles onto the functionalized surface of $Fe_3O_4@\beta$-CD results in even lower weight loss in the composite $Fe_3O_4@\beta$-CD@Pd (Figure 2D), indicating an increase in the inorganic component ratio. The amount of palladium in the composite is semi-quantitatively estimated to be 8.08% by comparing the mass loss of $Fe_3O_4@\beta$-CD and composite $Fe_3O_4@\beta$-CD@Pd, which is found to be in good agreement with the ICP-OES analysis result of 7.62% palladium content. The composite materials exhibit excellent stability at temperatures of 300 °C and above as there is no significant mass loss is observed.

The crystalline nature of the composite $Fe_3O_4@\beta$-CD@Pd is determined using XRD analysis. As shown in Figure 3, comparison between the XRD patterns of bare Fe_3O_4 (A), β-CD functionalized MNs $Fe_3O_4@\beta$-CD (B), and β-cyclodextrin functionalized Fe_3O_4-supported Pd nanoparticles $Fe_3O_4@\beta$-CD@Pd (C) is displayed to observe the sequential modification of Fe_3O_4. All composite materials (Figure 3A−C) exhibit characteristic peaks at 2θ = 30.2, 35.4, 43.2, 53.1, 57.2, and 62.7 corresponding to the reflections of (220), (311), (400), (422), (511), and (440).

The presence of these peaks indicates that the crystalline core structure of Fe_3O_4 remains unchanged in all composites, even after the functionalization with β-CD and deposition of palladium nanoparticles on the modified surface. This confirms that no phase transition occurred during the process and the
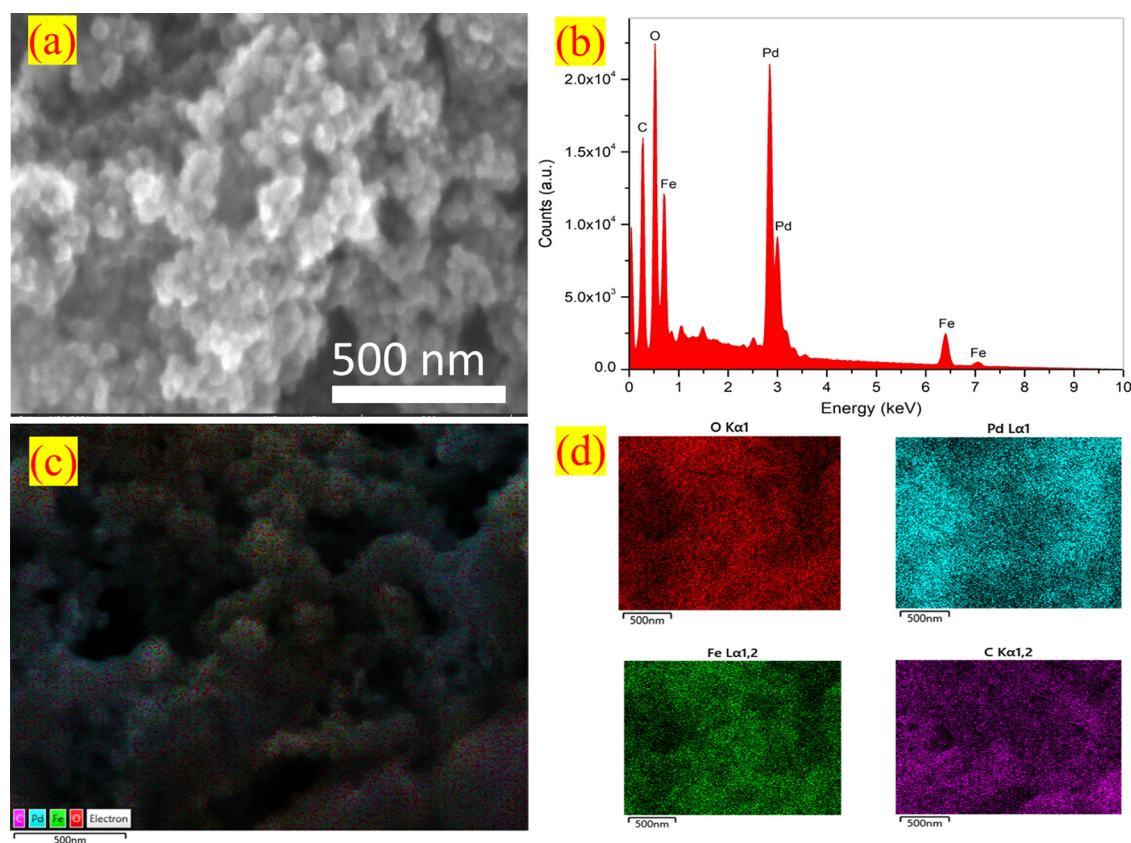
Figure 4. FE-SEM image and energy-dispersive X-ray spectrum (a and b; above) and energy dispersive X-ray (EDX) mapping (c and d; below) of $Fe_3O_4@$ β-CD@Pd.

functionalization of the surface of Fe_3O_4 with palladium nanoparticles. A similar behavior is observed in previously reported Fe_3O_4-based functionalized materials[43,44] and confirmed by the JCPDS card NO 75-1609 37.[45] Additionally, the XRD pattern of $Fe_3O_4@$ β-CD@Pd shows three extra peaks at $2\theta = 40.1$, 46.6, and 67.9 degrees, corresponding to the reflection of (111), (200), (111), and (220). The presence of these diffracted peaks confirms that the palladium nanoparticles are successfully deposited onto the β-CD functionalized surface of magnetic Fe_3O_4.[13]

The surface structure and morphology of the $Fe_3O_4@\beta$-CD@Pd composite materials is analyzed using field-emission scanning electron microscopy (FE-SEM). The FE-SEM image of the $Fe_3O_4@\beta$-CD@Pd material is captured before its use in catalytic reduction of nitroarenes reaction and represented in Figure 3a. Additionally, the energy dispersive X-ray (EDX) elemental composition and mapping spectra are studied during the FE-SEM image recording. Figure 4b,c exhibits the elemental composition EDX spectrum and mapping of the composite material $Fe_3O_4@\beta$-CD@Pd which clearly demonstrates that the magnetic Fe_3O_4 core is successfully functionalized with β-CD. The surface of the β-CD functionalized Fe_3O_4 is then further modified by the deposition of palladium nanoparticles on the same surface. In addition, EDX spectrum reveals that the palladium nanoparticles are evenly dispersed on the surface of the $Fe_3O_4@$ β-CD@Pd composite materials.

The transmission electron microscopy (TEM) technique is employed to investigate the physical characteristics of $Fe_3O_4@$ β-CD@Pd, such as its morphology, size, and crystallinity. The TEM image that is displayed in Figure 5a illustrates that the Fe_3O_4 nanoparticles are being coated onto an amorphous-
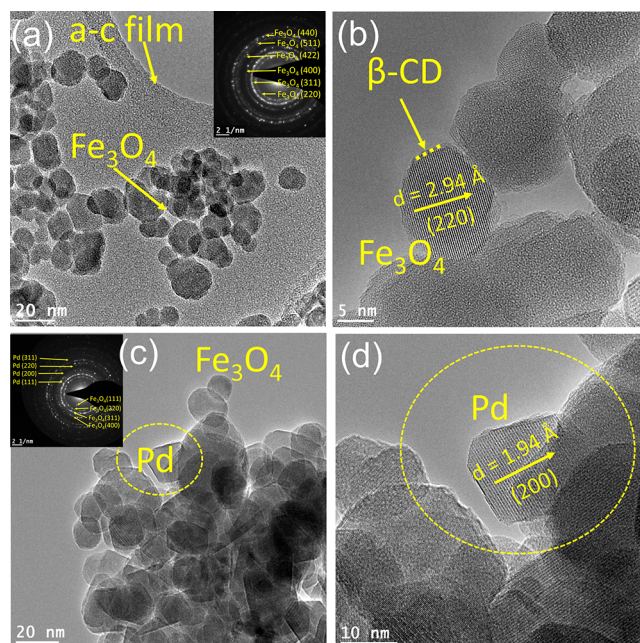

Figure 5. Bright field HRTEM micrographs showing (a) magnetic Fe_3O_4 (b) surface-modified magnetic $Fe_3O_4@\beta$-CD and (c) $Fe_3O_4@$ β-CD@Pd nanoparticles. The inset in (a) and (c) shows the SAED pattern. The encircled particle in (c) is shown in (d).

carbon film (a−c film) support. The nanoparticles appear to be evenly dispersed on the a-c film and comprise numerous nearly spherical particles based on the gray-scale contrasts. The
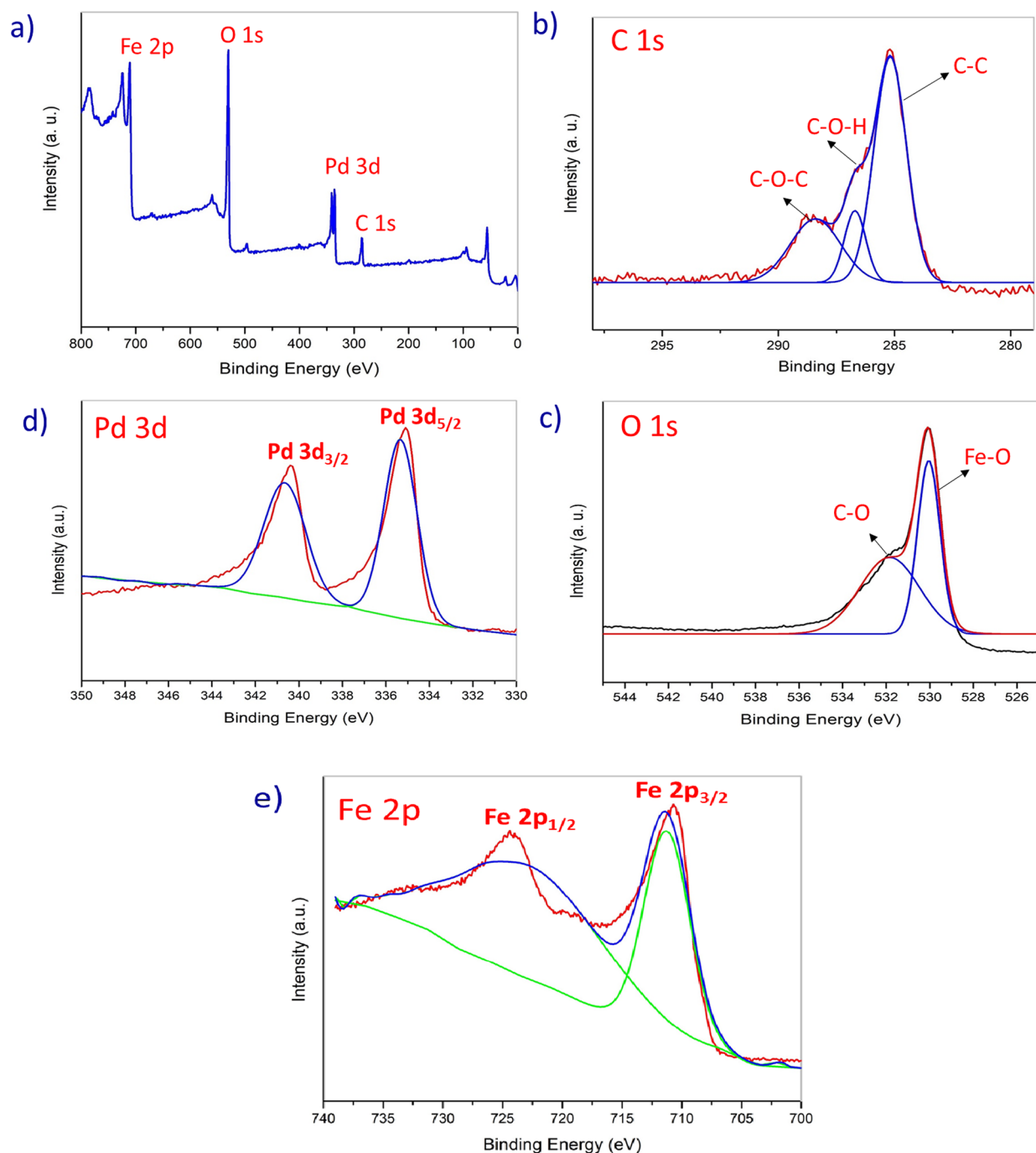
Figure 6. XPS spectra of (a) full range, (b) C 1s, (c) O 1s (d) Pd 3d, and (e) Fe 2p of $Fe_3O_4@\beta$-CD@Pd.

aggregation that is observed in this thin cluster could be attributed to the magnetic attraction between the nanoparticles. The statistical image analysis is used to determine the crystal size distribution and reveals an average size of 17 ± 3.5 nm (SI, Figure S2). Additionally, lattice-resolved images confirm that individual nanoparticle surfaces are free of any sheathed amorphous phase and are being clean and smooth. The selected area electron diffraction (SAED) pattern of Fe_3O_4 is displayed in the inset of the image in Figure 5a and indexed to the polycrystalline face centered cubic Fe_3O_4 [(400), (511), (422), (400), (311), and (220)] (JCPDS File No. 19-0629). Figure 5b presents TEM images of $Fe_3O_4@\beta$-CD particles, where the Fe_3O_4 nanoparticles are successfully grafted by the β-CD matrix with an interplanar spacing of 2.94 Å corresponding to the (220) plane of Fe_3O_4 being identified.

Figure 5c also displays TEM images of $Fe_3O_4@\beta$-CD@Pd nanoparticles, where the mixture contains aggregated Fe_3O_4 and Pd nanoparticles, and the Pd nanoparticles are attached to the β-Cd-functionalized $Fe_3O_4@\beta$-CD. The corresponding SAED pattern of the sample shows diffraction peaks consistent with the XRD analysis for both Fe_3O_4 and Pd nanoparticles. Figure 5c displays the SAED rings that are matched with the (111), (200), and (220) crystallographic planes of fcc-structured Pd nanoparticles (JCPDS file No. 87-0638). An interplanar spacing of 1.94 Å corresponding to the (200) plane of Pd is also identified (Figure 5d). The topotactic growth of Pd nanoparticles near the $Fe_3O_4@\beta$-CD matrix is demon-

Table 1. Optimization of the Reduction of 2-Nitroaniline Using $Fe_3O_4@\beta$-CD@Pd as the Catalyst[a]
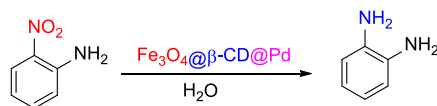
entry	catalyst	amount (mol % Pd)	temp. (°C)	hydrogen source	time (min)	yield[b]
1			RT	$NaBH_4$	60	trace
2	Fe_3O_4	10 mg	RT	$NaBH_4$	60	15
3	$Fe_3O_4@\ \beta$-CD	10 mg	RT	$NaBH_4$	60	30
4	$Fe_3O_4@\beta$-CD@Pd	10 mg (0.6)	RT	$NaBH_4$	60	75
5	$Fe_3O_4@\beta$-CD@Pd	10 mg (0.6)	RT	HCOOH	60	
6	$Fe_3O_4@\beta$-CD@Pd	10 mg (0.6)	RT	HCOONa	60	
7	$Fe_3O_4@\beta$-CD@Pd	10 mg (0.6)	RT	$N_2H_4\ H_2O$	60	
8	$Fe_3O_4@\beta$-CD@Pd	10 mg (0.6)	RT	isopropanol	60	18
9	$Fe_3O_4@\beta$-CD@Pd	10 mg (0.6)	50 °C	$NaBH_4$	60	99
10	$Fe_3O_4@\beta$-CD@Pd	10 mg (0.6)	50 °C	$NaBH_4$	40	99
11	$Fe_3O_4@\beta$-CD@Pd	10 mg (0.6)	50 °C	$NaBH_4$	30	99
12	$Fe_3O_4@\beta$-CD@Pd	10 mg (0.6)	50 °C	$NaBH_4$	20	90
13	$Fe_3O_4@\beta$-CD@Pd	5 mg (0.3)	50 °C	$NaBH_4$	30	99
14	$Fe_3O_4@\beta$-CD@Pd	3 mg (0.2)	50 °C	$NaBH_4$	30	95
15	$Fe_3O_4@\beta$-CD@Pd	5 mg (0.3)	50 °C	$NaBH_4$	30	60[c]

[a]Reaction conditions: 2-nitroaniline (1.0 mmol), H_2O (3.0 mL) as the solvent, hydrogen donor (2.0 mmol), and catalyst $Fe_3O_4@\beta$-CD@Pd. [b]Yield was determined using GC−MS. [c]Neat condition.

strated through HRTEM observation and SAED analysis.[46] The TEM image of $Fe_3O_4@\beta$-CD@Pd after the fifth catalytic cycle of nitroarene reduction is presented in Figure 9 along with the corresponding SAED pattern exhibiting diffraction peaks of Fe_3O_4 and Pd nanoparticles that are aligned with the originally synthesized particles. No significant alterations in the structure or morphology of the catalyst $Fe_3O_4@\beta$-CD@Pd are detected after the fifth catalytic cycle (Figure 9).

The surface composition and chemical nature of the catalyst $Fe_3O_4@\beta$-CD@Pd are evaluated by the XPS analysis. Figure 6a exhibits the full range XPS survey of $Fe_3O_4@\beta$-CD@Pd which indicates the presence of expected C (286. 3 eV), Pd (337.9 eV), O (530.9 eV), and Fe (717.1 eV) elements in the catalyst material. The high-resolution XPS curve of carbon (Figure 6b) reveals three characteristic peaks at 285.2, 286. 7, and 288.4 eV in the C 1s region corresponding to the C−C, C−OH, and C−O−C bond, which indicates the successful functionalization of Fe_3O_4 with the β-cyclodextrin moiety.[47] Figure 6c shows the XPS curve of O 1s and appearance of two peaks at 530.0 and 531.8 eV which are responsible for Fe−O and C−O bonds, respectively. The successful deposition of Pd nanoparticles on the surface of β-CD-functionalized Fe_3O_4 is confirmed by the high regulation XPS in the range of 330 to 350 eV (Figure 6d). The binding energies 335.57 and 340.3 eV are attributed for Pd $3d_{5/2}$ and Pd $3d_{3/2}$, respectively. These two intense peaks confirm the efficient formation of Pd nanoparticles on the surface of the materials.

This observation has close resemblance with the reported literature result.[48] Figure 6e represents the Fe 2p scan of $Fe_3O_4@\beta$-CD@Pd materials which exhibit two peaks at 710.6 and 723.6 eV, respectively. The appearance of these two binding energy peaks is indicative of Fe $2p_{3/2}$ and Fe $2p_{1/2}$, which confirms the presence of the Fe_3O_4 core in the material $Fe_3O_4@\beta$-CD@Pd.[49]

After completing the state-of-art characterization of $Fe_3O_4@\beta$-CD@Pd through employing various techniques such as FTIR, TGA, XRD FE-SEM, EDX, TEM, and XPS, the precise amount of palladium content present on the catalyst has been

estimated using ICP-OES analysis. The results from the ICP-OES analysis reveal that the $Fe_3O_4@\beta$-CD@Pd catalyst material has a palladium loading of 7.62% (w/w) or 0.72 mmol/g. Even in 1.04 g scale of ICP-OES analysis, the $Fe_3O_4@\beta$-CD@Pd shows the same 0.72 mmol/g palladium loaded in the materials. The details of the experimental procedure for ICP-OES analysis for the determination of palladium content in the catalyst material can be found in Section 5 of the Supporting Information. All the physicochemical characterization techniques which are used confirm that Pd nanoparticles are effectively deposited on the β-CD-functionalized surface of magnetic $Fe_3O_4@\beta$-CD.
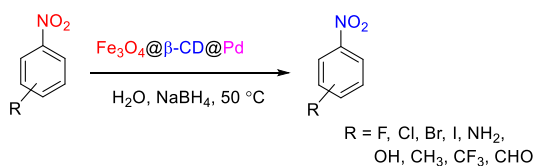
3.2. Catalytic Activity of $Fe_3O_4@\beta$-CD@Pd for the Reduction of Nitroarenes. After completing the state-of-art characterization, the catalytic activity of $Fe_3O_4@\beta$-CD@Pd is investigated for the reduction of nitro compounds. Initially, 2-nitroaniline is chosen as the standard substrate for the reduction reaction employing $Fe_3O_4@\beta$-CD@Pd as the catalyst. The results for the optimization of catalyst screening by varying the parameters such as catalyst loadings, temperature, hydrogen source, and reaction times for the reduction of 2-nitroaniline are summarized in Table 1. The reaction progress is monitored by thin layer chromatography (TLC). The conversion and product yield are determined by gas chromatography−mass spectrometry (GC−MS). Initially, the reduction reaction is carried out in an aqueous medium in the absence of $Fe_3O_4@\beta$-CD@Pd to check whether the reduction reaction proceeded without the catalyst. Noticeably, 2-nitroaniline is converted to only a trace amount of the desired product after 60 min of stirring at room temperature in the presence of 2.0 equivalent of $NaBH_4$ (Table 1, entry 1). However, 15−30% of the products are obtained in the presence of 10.0 mg of bare Fe_3O_4 and β-CD functionalized $Fe_3O_4@\beta$-CD (Table 1, entries 2−3) under the same reaction conditions. Remarkably, the product yield is increased to 75%, while 10.0 mg (0.6 mol % Pd) of $Fe_3O_4@\beta$-CD@Pd has been used under the same investigated conditions (Table 1, entry 4). For verifying the compatibility of the use of hydrogen

source, no detectable amounts of the desired products are obtained when HCOOH, HCOONa, and $N_2H_4 \cdot H_2O$ and $NaHCO_3$ are used instead of $NaBH_4$ (Table 1, entries 5−7). However, only 18% of the desired benzene-1,2-dimanie is detected using isopropanol as the hydrogen source under the same investigation conditions (Table 1, entry 8). Therefore, $NaBH_4$ is the effective hydrogen source for the reduction of 2-nitroaniline in the presence of $Fe_3O_4@\beta$-CD@Pd as the catalyst. Remarkably, in the same reaction, upon heating at 50 °C for 60 min, the yield significantly increases to 99% (Table 1, entry 9). The product yield remains at 99% even when the heating time decreases to 40 and 30 min, respectively (Table 1, entries 10−11). However, further decrease in the heating time to 20 min lowers the product yield to 90% (Table 1, entry 12). For optimizing the catalyst loading, lowering the amount of $Fe_3O_4@\beta$-CD@Pd from 10.0 to 5.0 mg (0.3 mol % Pd) produces the same 99% of the desired product (Table 1, entry 13). Further decrease in the catalyst loading to 3.0 mg lowers the product yield to 95% (Table 1, entry 14). To check the requirement of solvent H_2O for the reduction of 2-nitroaniline, neat reaction condition produces only 60% of the desired product (Table 1, entry 15).

After optimizing the reduction of 2-nitroanilne, the further applicability of the $Fe_3O_4@\beta$-CD@Pd catalyst is explored to other nitroarenes reduction reactions. Substrate scope of nitroarenes reduction using $Fe_3O_4@\beta$-CD@Pd is summarized in Table 2. Five milligrams (0.3 mol % Pd) of $Fe_3O_4@\beta$-CD@Pd reduce nitrobenzene to aniline very efficiently (99%) in the presence of 2.0 equiv of $NaBH_4$ in water (Table 2, entry 1). Nitrobenzene with electron-withdrawing group substituents (I, Br, Cl, and F) produces a high yield of desired amine products under the same reaction conditions (Table 2, entries 2−5). Nitrobenzene with electron-donating group substituents such as $-NH_2$ also produces excellent yield of diamines (Table 2, entries 6−8). Nitrobenzene with both electron-withdrawing and -donating groups such as $-Br$ and $-CH_3$ containing 1-bromo-2-methyl-4-nitrobenzene reduces to corresponding 4-bromo-3-methylaniline in 98% yield (Table 2, entry 9). Nitrobenzene with both electron-donating groups such as $-NH_2$ and $-CH_3$ containing 4-methyl-2-nitroaniline also produces excellent yield of the desired 4-methylbenzene-1,2-diamine under the same experimental conditions (Table 2, entry 11). Nitrobenzene with other substituents such as $-CF_3$, $-OH$, and $-CHO$ containing nitroarenes also produce an excellent amount of the corresponding desired products (Table 2, entries 10, 11, and 13). Overall, the catalyst $Fe_3O_4@\beta$-CD@Pd shows an excellent reducing performance for the reduction of a variety of nitroarenes in water at 50 °C within 0.5 h. A comparison of the catalytic performance of current $Fe_3O_4@\beta$-CD@Pd is compared with the previously reported Fe_3O_4-based catalysts for the reduction of nitroarenes. The comparison results are summarized in Table 3.

3.3. Determination of the Heterogenous Nature of the Catalyst $Fe_3O_4@\beta$-CD@Pd. The actual nature of the catalyst in the optimized reaction conditions is determined by conducting a hot filtration test. To know whether the catalyst $Fe_3O_4@\beta$-CD@Pd is truly heterogeneous or homogenous in reaction media, a control catalytic reduction experiment is conducted for 2-nitroaniline. After 10.0 min of the reaction, the solid magnetic catalyst $Fe_3O_4@\beta$-CD@Pd is separated with an external magnet, and then, the clear solution part of the reaction mixture is continuously stirred for 30 more minutes at 50 °C. As shown in Figure 7, the product yield remained

**Table 2. Substrate Scope for the Reduction of Different Nitroarenes Using $Fe_3O_4@\beta$-CD@Pd as the Catalyst[a]**

R = F, Cl, Br, I, NH_2, OH, CH_3, CF_3, CHO

Entry	Substrate	Product	Yield (%)[b]	TON[c]	TOF[d]
1			99	330	660
2			99	330	660
3			98	327	653
4			98	327	653
5			99	330	660
6			95	316	632
7			99	330	660
8			97	323	646
9			98	327	653
10			98	327	653
11			96	320	640
12			98	327	653
13			97	323	646

[a]Reaction condition: Nitroarene (1.0 mmol), catalysts $Fe_3O_4@\beta$-CD@Pd (5.0 mg; 0.3 mol % Pd), solvent H_2O (3.0 mL), $NaBH_4$ (2.0 mmol), stirred at room temperature. [b]Yield (%) is measured by GC−MS. [c]Turnover Number (TON) = number of moles of product/number of moles of catalyst. [d]Turnover Frequency (TOF) = number of moles of product formed per mole of catalyst/hour.

Table 3. Comparison of the Catalytic Activity of Fe₃O₄@β-CD@Pd with Other Fe₃O₄-Based Catalysts for the Reduction of Nitroarenes

| entry	catalyst (amount; mol)	substrate	reaction conditions	time	yield %	ref
1	Fe$_3$O$_4$@Cu (5.0 wt %)	2-nitroaniline	MeOH, RT, 5.0 wt % of catalyst, 3.0 mmol NaBH$_4$	90 min	99	50
2	Fe$_3$O$_4$@Guanidine-Pd (0.13 mol %)	4-nitroaniline	H$_2$O, RT, 2.0 mmol NaBH$_4$	40 min	96	51
3	Pd-GO/CNT—Fe$_3$O$_4$ (1.0 mol %)	nitrobenzene	H$_2$O, H$_2$ (1.0 atm), 60 °C	180 min	90	52
4	Fe$_3$O$_4$-pRGO@Ag (10 wt %; 6.5 mol % Ag)	nitrobenzene	2-propanol, KOH (3.0 mmol), 1000 °C	24 h	96	53
5	C—Pd—Fe$_3$O$_4$ (20 mg)	nitrobenzene	EtOH, NaBH$_4$ (3.0 mmol), 25 °C	30 min	99	54
6	Fe$_3$O$_4$@NC@Pt (0.5 mol %)	2-nitroaniline	Toluene (3.0 mL), N$_2$H$_4$ H$_2$O (4.0 mmol), 70 °C	4 h	94	55
7	Fe$_3$O$_4$@SiO$_2$/Schif base/Pd(II) (0.52 mol %)	2-nitroaniline	EtOH (3.0 mL), N$_2$H$_4$ H$_2$O (3.0 mmol), 80 °C	1.83 h	94	56
8	Fe$_3$O$_4$@Cu(OH) × (10.0 mol %)	2-nitroaniline	H$_2$O (3.0 mL), NaBH$_4$ (2.0 mmol), 60 °C	5.0 min	91	57
9	Fe$_3$O$_4$@C—Pd (40 mg)	nitrobenzene	NaBH$_4$ (3 mmol), EtOH, 25 °C	60 min	99	58
10	Fe$_3$O$_4$@β-CD@Pd (0.3 mol % Pd)	2-nitroaniline	H$_2$O, NaBH$_4$ (2.0 mmol), 50 °C	30 min	99	present work
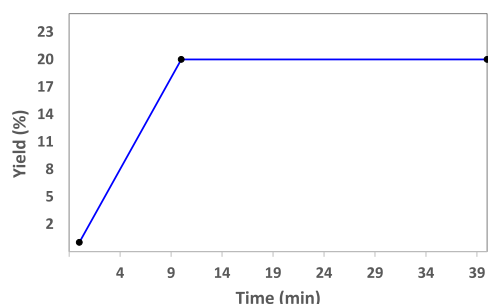
Figure 7. Hot filtration test of the catalyst for the catalytic reduction of 2-nitroaniline. Conditions: 2-Nitroaniline (1.0 mmol), H$_2$O (3.0 mL) as the solvent, NaBH$_4$ (2.0 mmol), and catalyst Fe$_3$O$_4$@β-CD@Pd (0.3 mol % Pd), 50 ° C.

Figure 8. Reusability of the catalyst Fe$_3$O$_4$@β-CD@Pd for the catalytic reduction of 2-nitroaniline. Conditions: 2-nitroaniline (1.0 mmol), H$_2$O (3.0 mL) as the solvent, NaBH$_4$ (2.0 mmol), and catalyst Fe$_3$O$_4$@β-CD@Pd (0.3 mol % Pd), 50 ° C.

constant after the removal of the solid catalyst from the reaction mixture (GC traces and mass spectra of the reaction are provided in the SI, section 8). This result concludes that no detectable Pd has been leached out from the catalyst during the reduction of nitro compounds and the catalyst remains in the heterogeneous state.

Putting together these observations prove that the catalyst that is used in the reduction of nitroarene reaction is indeed heterogeneous and that no detectable Pd has been leached out during the reaction. Furthermore, ICP-OES analysis of the used catalyst reveals palladium content 7.60% (w/w) or 0.71 mmol/g, which is almost like the original value of 7.62% or 0.72 mmol/g.

3.4. Reusability of the Catalyst Fe₃O₄@β-CD@Pd. Generally, the Fe$_3$O$_4$-based heterogeneous catalyst offers a significant advantage in industrial applications due to its effortless separation from the reaction mixture using an external magnet, which is straightforward and uncomplicated compared to other available processes. Therefore, this easy magnetic separation capability makes the Fe$_3$O$_4$-based catalyst a very attractive option for recycling and reusable in the catalytic reaction in organic transformations. In this study, the recycling and reusability of the catalyst Fe$_3$O$_4$@β-CD@Pd are examined in the reduction of 2-nitroaniline to benzene-1,2-diamine in the presence of NaBH$_4$ under optimal conditions (Figure 8). After each cycle, the catalyst is retrieved by the external magnet and then washed with ethanol multiple times and dried under vacuum.

The recovered catalyst is estimated after each cycle of the reaction and found to be the same original amount 5.0 mg (0.3 mol % of Pd) of Fe$_3$O$_4$@β-CD@Pd. The catalyst is used for up
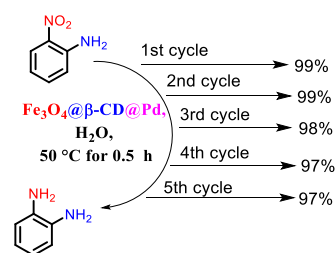
to five cycles for the reduction of 2-nitroaniline, and no significant loss of catalytic activity (97%) is found.

In addition to that, other characterizations of the used catalyst including TEM, FE-SEM (SI, S1), and XRD show the same chemical and morphological properties as before. Figure 9 shows the bright field HRTEM micrographs (a), SAED pattern (b), FE-SEM image (c), and XRD pattern (A; bare Fe$_3$O$_4$ and B; Fe$_3$O$_4$@β-CD@Pd) (d) of the catalyst Fe$_3$O$_4$@β-CD@Pd after the 5th cycle of the catalytic reaction.
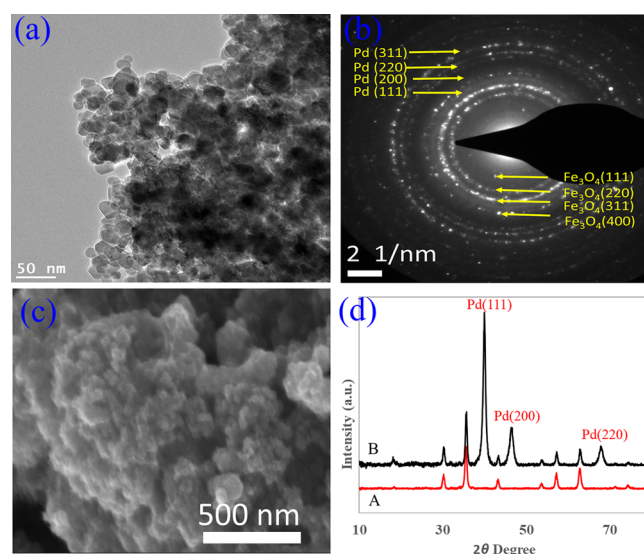
Figure 9. Bright field HRTEM micrographs (a), SAED pattern (b), FE-SEM image (c), and XRD pattern (A; bare Fe$_3$O$_4$ and B; Fe$_3$O$_4$@β-CD@Pd) (d) of the catalyst Fe$_3$O$_4$@β-CD@Pd after the 5th cycle of the catalytic reaction.

4. CONCLUSIONS

In conclusion, a highly effective magnetic heterogeneous catalyst $Fe_3O_4@\beta$-CD@Pd has been synthesized and thoroughly characterized using cutting-edge techniques. The catalyst exhibits exceptional catalytic activity for the reduction of nitroarenes in water at 50 °C with the aid of $NaBH_4$. A wide range of nitroarenes with varying substituents, including both electron-withdrawing (I, Br, Cl, F, CF_3, CHO) and electron-releasing groups (NH_2, CH_3), can be reduced using this catalyst. Additionally, $Fe_3O_4@\beta$-CD@Pd is magnetic and can be easily separated from the reaction mixture and can be reused up to five times without a significant loss in catalytic performance. This catalyst is made from environmentally friendly materials, including the Fe_3O_4 core and the bio-renewable feedstock β-CD. As a result, $Fe_3O_4@\beta$-CD@Pd can be employed in sustainable and cost-effective nitroarenes reduction reactions.

■ ASSOCIATED CONTENT

Ⓢ Supporting Information

The Supporting Information is available free of charge at https://pubs.acs.org/doi/10.1021/acsomega.3c02332.

> FE-SEM and EDS of $Fe_3O_4@\beta$-CD@Pd after the 5th catalytic cycle; TEM of bare Fe_3O_4; details procedure of the determination of Pd content in the catalyst materials by ICP-OES; GC traces and mass spectra of the products for optimization of the catalytic condition and substrate screening; ^1H and ^{13}C NMR chemical shift and the spectra; and GC traces and mass spectra of the products for the hot gravity filtration test and reusability of the $Fe_3O_4@\beta$-CD@Pd (PDF)

■ AUTHOR INFORMATION

Corresponding Author

Kamrul Hasan − *Department of Chemistry, Pure and Applied Chemistry Group, College of Sciences, University of Sharjah, Sharjah 27272, United Arab Emirates;* ⓞ orcid.org/0000-0003-4268-6381; Email: khasan@sharjah.ac.ae

Authors

Ihsan A. Shehadi − *Department of Chemistry, Pure and Applied Chemistry Group, College of Sciences, University of Sharjah, Sharjah 27272, United Arab Emirates*

Reshma G. Joseph − *Department of Chemistry, Pure and Applied Chemistry Group, College of Sciences, University of Sharjah, Sharjah 27272, United Arab Emirates*

Shashikant P. Patole − *Department of Physics, Khalifa University of Science and Technology, Abu Dhabi 127788, United Arab Emirates;* ⓞ orcid.org/0000-0001-6669-6635

Abdelaziz Elgamouz − *Department of Chemistry, Pure and Applied Chemistry Group, College of Sciences, University of Sharjah, Sharjah 27272, United Arab Emirates;* ⓞ orcid.org/0000-0002-6667-7511

Complete contact information is available at:
https://pubs.acs.org/10.1021/acsomega.3c02332

Notes

The authors declare no competing financial interest.

■ REFERENCES

(1) Khaleel, A.; Shehadi, I.; Al-Marzouqi, A. J. F. Catalytic conversion of chloromethane to methanol and dimethyl ether over mesoporous γ-alumina. *Fuel Process. Technol.* **2011**, *92*, 1783−1789.

(2) Wang, H.; Yan, S.; Qu, B.; Liu, H.; Ding, J.; Ren, N. Magnetic solid phase extraction using $Fe_3O_4@\beta$-cyclodextrin−lipid bilayers as adsorbents followed by GC-QTOF-MS for the analysis of nine pesticides. *New J. Chem.* **2020**, *44*, 7727−7739.

(3) Pooresmaeil, M.; Namazi, H. β-Cyclodextrin grafted magnetic graphene oxide applicable as cancer drug delivery agent: Synthesis and characterization. *Mater. Chem. Phys.* **2018**, *218*, 62−69.

(4) Khaleel, A.; Shehadi, I.; Al-Shamisi, M. J. J. Structural and textural characterization of sol−gel prepared nanoscale titanium−chromium mixed oxides. *J. Non-Cryst. Solids* **2010**, *356*, 1282−1287.

(5) Al-Marzouqi, A. H.; Elwy, H. M.; Shehadi, I.; Adem, A. Physicochemical properties of antifungal drug-cyclodextrin complexes prepared by supercritical carbon dioxide and by conventional techniques. *J. Pharm. Biomed. Anal.* **2009**, *49*, 227−233.

(6) de Souza, J. F.; da Silva, G. T.; Fajardo, A. R. Chitosan-based film supported copper nanoparticles: A potential and reusable catalyst for the reduction of aromatic nitro compounds. *Carbohydr. Polym.* **2017**, *161*, 187−196.

(7) Rana, M. S.; Halim, M. A.; Hoque, S. A. M. W.; Hasan, K.; Hossain, M. K. Bioadsorbtion of arsenic by prepared and commercial crab shell chitosan. *Biotechnology* **2008**, *8*, 160−165.

(8) Liu, Y.; Hartman, R. L. Reaction kinetics of a water-soluble palladium−β-cyclodextrin catalyst for a Suzuki−Miyaura cross-coupling in continuous flow. *React. Chem. Eng.* **2019**, *4*, 1341−1346.

(9) Luo, K.; Zhang, L.; Yang, R.; Jin, Y.; Lin, J. Picolinamide modified β-cyclodextrin/Pd (II) complex: Asupramolecular catalyst for Suzuki-Miyaura coupling of aryl, benzyl and allyl halides with arylboronic acids in water. *Carbohydr. Polym.* **2018**, *200*, 200−210.

(10) Mirhosseyni, M. S.; Nemati, F. Fe/N co-doped mesoporous carbon derived from cellulose-based ionic liquid as an efficient heterogeneous catalyst toward nitro aromatic compound reduction reaction. *Int. J. Biol. Macromol.* **2021**, *175*, 432−442.

(11) Bromho, T. K.; Ibrahim, K.; Kabir, H.; Rahman, M. M.; Hasan, K.; Ferdous, T.; Taha, H.; Altarawneh, M.; Jiang, Z. T. Understanding the impacts of Al+3-substitutions on the enhancement of magnetic, dielectric and electrical behaviors of ceramic processed nickel-zinc mixed ferrites: FTIR assisted studies. *Mater. Res. Bull.* **2018**, *97*, 444−451.

(12) Tabasso, S.; Calcio Gaudino, E.; Acciardo, E.; Manzoli, M.; Bonelli, B.; Cravotto, G. Microwave-Assisted Protocol for Green Functionalization of Thiophenes With a Pd/β-Cyclodextrin Cross-Linked Nanocatalyst. *Front. Chem.* **2020**, *8*, 253.

(13) Tabasso, S.; Calcio Gaudino, E.; Acciardo, E.; Manzoli, M.; Giacomino, A.; Cravotto, G. J. M. Microwave-Assisted Dehydrogenative Cross Coupling Reactions in γ-valerolactone with a reusable Pd/β-cyclodextrin crosslinked catalyst. *Molecules* **2019**, *24*, 288.

(14) Zare Asadabadi, A.; Hoseini, S. J.; Bahrami, M.; Nabavizadeh, S. M. Catalytic applications of β-cyclodextrin/palladium nanoparticle thin film obtained from oil/water interface in the reduction of toxic nitrophenol compounds and the degradation of azo dyes. *New J. Chem.* **2019**, *43*, 6513−6522.

(15) Panigrahi, S.; Basu, S.; Praharaj, S.; Pande, S.; Jana, S.; Pal, A.; Ghosh, S. K.; Pal, T. Synthesis and Size-Selective Catalysis by

Supported Gold Nanoparticles: Study on Heterogeneous and Homogeneous Catalytic Process. *J. Phys. Chem. C* 2007, *111*, 4596−4605.

(16) Spain, J. C. Biodegradation of Nitroaromatic Compounds. *Annu. Rev. Microbiol.* 1995, *49*, 523−555.

(17) Shen, J.; He, R.; Wang, L.; Zhang, J.; Zuo, Y.; Li, Y.; Sun, X.; Li, J.; Han, W. Biodegradation kinetics of picric acid by Rhodococcus sp.NJUST16 in batch reactors. *J. Hazard. Mater.* 2009, *167*, 193−198.

(18) Shahriari, M.; Ali Hosseini Sedigh, M.; Shahriari, M.; Stenzel, M.; Mahdi Zangeneh, M.; Zangeneh, A.; Mahdavi, B.; Asadnia, M.; Gholami, J.; Karmakar, B.; Veisi, H. Palladium nanoparticles decorated Chitosan-Pectin modified Kaolin: It's catalytic activity for Suzuki-Miyaura coupling reaction, reduction of the 4-nitrophenol, and treatment of lung cancer. *Inorg. Chem. Commun.* 2022, *141*, No. 109523.

(19) Hamelian, M.; Varmira, K.; Karmakar, B.; Veisi, H. Catalytic Reduction of 4-Nitrophenol Using Green Synthesized Silver and Gold Nanoparticles over Thyme Plant Extract. *Catal. Lett.* 2022, DOI: 10.1007/s10562-022-04164-3.

(20) Veisi, H.; Joshani, Z.; Karmakar, B.; Tamoradi, T.; Heravi, M. M.; Gholami, J. Ultrasound assisted synthesis of Pd NPs decorated chitosan-starch functionalized Fe3O4 nanocomposite catalyst towards Suzuki-Miyaura coupling and reduction of 4-nitrophenol. *Int. J. Biol. Macromol.* 2021, *172*, 104−113.

(21) Hemmati, S.; Heravi, M. M.; Karmakar, B.; Veisi, H. In situ decoration of Au NPs over polydopamine encapsulated GO/Fe(3)O(4) nanoparticles as a recyclable nanocatalyst for the reduction of nitroarenes. *Sci. Rep.* 2021, *11*, 12362.

(22) Ghorbani-Vaghei, R.; Veisi, H.; Aliani, M. H.; Mohammadi, P.; Karmakar, B. Alginate modified magnetic nanoparticles to immobilization of gold nanoparticles as an efficient magnetic nanocatalyst for reduction of 4-nitrophenol in water. *J. Mol. Liq.* 2021, *327*, No. 114868.

(23) Veisi, H.; Ozturk, T.; Karmakar, B.; Tamoradi, T.; Hemmati, S. In situ decorated Pd NPs on chitosan-encapsulated Fe3O4/SiO2-NH2 as magnetic catalyst in Suzuki-Miyaura coupling and 4-nitrophenol reduction. *Carbohydr. Polym.* 2020, *235*, No. 115966.

(24) Yazdankhah, M.; Veisi, H.; Hemmati, S. In situ immobilized palladium nanoparticles (Pd NPs) on fritillaria imperialis flower extract-modified graphene and their catalytic activity for reduction of 4-nitrophenol. *J. Taiwan Inst. Chem. Eng.* 2018, *91*, 38−46.

(25) Krogul-Sobczak, A.; Cedrowski, J.; Kasperska, P.; Litwinienko, G. Reduction of Nitrobenzene to Aniline by CO/H2O in the Presence of Palladium Nanoparticles. *Catalysts* 2019, *9*, 404.

(26) Guo, Z.; Li, Y.; Pan, S.; Xu, J. Fabrication of Fe3O4@cyclodextrin magnetic composite for the high-efficient removal of Eu(III). *J. Mol. Liq.* 2015, *206*, 272−277.

(27) Hasan, K.; Zysman-Colman, E. The Effect of Aryl Substitution on the Properties of a Series of Highly Absorptive Cationic Iridium(III) Complexes Bearing Ancillary Bis(arylimino)-acenaphthene Ligands. *Eur. J. Inorg. Chem.* 2013, *2013*, 4421−4429.

(28) Zhou, J.; Dong, Z.; Yang, H.; Shi, Z.; Zhou, X.; Li, R. Pd immobilized on magnetic chitosan as a heterogeneous catalyst for acetalization and hydrogenation reactions. *Appl. Surf. Sci.* 2013, *279*, 360−366.

(29) Sardarian, A. R.; Dindarloo Inaloo, I.; Zangiabadi, M. An Fe3O4@SiO2/Schiff base/Cu(ii) complex as an efficient recyclable magnetic nanocatalyst for selective mono N-arylation of primary O-alkyl thiocarbamates and primary O-alkyl carbamates with aryl halides and arylboronic acids. *New J. Chem.* 2019, *43*, 8557−8565.

(30) Sardarian, A. R.; Zangiabadi, M.; Inaloo, I. D. Fe3O4@SiO2/Schiff base/Pd complex as an efficient heterogeneous and recyclable nanocatalyst for chemoselective N-arylation of O-alkyl primary carbamates. *RSC Adv.* 2016, *6*, 92057−92064.

(31) Dindarloo Inaloo, I.; Majnooni, S.; Eslahi, H.; Esmaeilpour, M. Efficient nickel(II) immobilized on EDTA-modified $Fe_3O_4@SiO_2$ nanospheres as a novel nanocatalyst for amination of heteroaryl carbamates and sulfamates through the cleavage of C-O bond. *Mol. Catal.* 2020, *492*, No. 110915.

(32) Inaloo, I. D.; Majnooni, S. A Fe3O4@SiO2/Schiff Base/Pd Complex as an Efficient Heterogeneous and Recyclable Nanocatalyst for One-Pot Domino Synthesis of Carbamates and Unsymmetrical Ureas. *Eur. J. Org. Chem.* 2019, *2019*, 6359−6368.

(33) Hasan, K.; Shehadi, I. A.; Al-Bab, N. D.; Elgamouz, A. Magnetic chitosan-supported silver nanoparticles: A heterogeneous catalyst for the reduction of 4-nitrophenol. *Catalysts* 2019, *9*, 839.

(34) Hasan, K.; Shehadi, I. A.; Ahmed Bagudu, K.; Osama Mohamed Elmabrouk, N.; Elgamouz, A.; Patole, S. P.; Al-Qawasmeh, R. A. Magnetic silica surface functionalized palladium catalyst: A modular approach for C−C cross-coupling reactions in water. *Appl. Surf. Sci.* 2022, *571*, No. 151369.

(35) Hasan, K. Methyl Salicylate Functionalized Magnetic Chitosan Immobilized Palladium Nanoparticles: An Efficient Catalyst for the Suzuki and Heck Coupling Reactions in Water. *ChemistrySelect* 2020, *5*, 7129−7140.

(36) Hasan, K.; Joseph, R. G.; Patole, S. P. Copper Pyrrole-imine Incorporated Fe3O4-Nanocomposite: A Magnetically Separable and Reusable Catalyst for the Oxidative Amination of Aryl Aldehydes. *ChemistrySelect* 2022, *7*, No. e202201840.

(37) Hasan, K.; Joseph, R. G.; Patole, S. P.; Al-Qawasmeh, R. A. Development of magnetic Fe3O4-chitosan immobilized Cu(II) Schiff base catalyst: An efficient and reusable catalyst for microwave assisted one-pot synthesis of propargylamines via A3 coupling. *Catal. Commun.* 2023, *174*, No. 106588.

(38) Ahmad, I.; Shagufta; Dhar, R.; Hisaindee, S.; Hasan, K. An Environmentally Benign Solid Acid Nanocatalyst for the Green Synthesis of Carboxylic Acid Ester. *ChemistrySelect* 2021, *6*, 9645−9652.

(39) Wang, H.-B.; Zhang, Y.-H.; Zhang, Y.-B.; Zhang, F.-W.; Niu, J.-R.; Yang, H.-L.; Li, R.; Ma, J.-T. Pd immobilized on thiol-modified magnetic nanoparticles: A complete magnetically recoverable and highly active catalyst for hydrogenation reactions. *Solid State Sci.* 2012, *14*, 1256−1262.

(40) Ma, Y.-X.; Shao, W.-J.; Sun, W.; Kou, Y.-L.; Li, X.; Yang, H.-P. One-step fabrication of β-cyclodextrin modified magnetic graphene oxide nanohybrids for adsorption of Pb(II), Cu(II) and methylene blue in aqueous solutions. *Appl. Surf. Sci.* 2018, *459*, 544−553.

(41) Mullassery, M. D.; Fernandez, N. B.; Surya, R.; Thomas, D. Microwave- assisted green synthesis of acrylamide cyclodextrin-grafted silylated bentonite for the controlled delivery of tetracycline hydrochloride. *Sustainable Chem. Pharm.* 2018, *10*, 103−111.

(42) Feiz, A.; Loni, M.; Naderi, S.; Bazgir, A. The β-cyclodextrin decorated with palladium nanoparticles without pretreatment: An efficient heterogeneous catalyst for biaryls synthesis. *Appl. Organomet. Chem.* 2018, *32*, No. e4608.

(43) Safari, J.; Javadian, L. Chitosan decorated Fe3O4 nanoparticles as a magnetic catalyst in the synthesis of phenytoin derivatives. *RSC Adv.* 2014, *4*, 48973−48979.

(44) Zhang, L.-Y.; Zhu, X.-J.; Sun, H.-W.; Chi, G.-R.; Xu, J.-X.; Sun, Y.-L. Control synthesis of magnetic Fe3O4−chitosan nanoparticles under UV irradiation in aqueous system. *Curr. Appl. Phys.* 2010, *10*, 828−833.

(45) Deng, H.; Li, X.; Peng, Q.; Wang, X.; Chen, J.; Li, Y. Monodisperse magnetic single-crystal ferrite microspheres. *Angew. Chem., Int. Ed.* 2005, *44*, 2782−2785.

(46) Putta, C.; Sharavath, V.; Sarkar, S.; Ghosh, S. Palladium nanoparticles on β-cyclodextrin functionalised graphene nanosheets: a supramolecular based heterogeneous catalyst for C−C coupling reactions under green reaction conditions. *RSC Adv.* 2015, *5*, 6652−6660.

(47) Veisi, H.; Najafi, S.; Hemmati, S. Pd(II)/Pd(0) anchored to magnetic nanoparticles (Fe3O4) modified with biguanidine-chitosan polymer as a novel nanocatalyst for Suzuki-Miyaura coupling reactions. *Int. J. Biol. Macromol.* 2018, *113*, 186−194.

(48) Sun, W.; Yang, W.; Xu, Z.; Li, Q. Anchoring Pd Nanoparticles on Fe3O4@SiO2 Core−Shell Nanoparticles by Cross-Linked Polyvinylpyrrolidone for Nitrite Reduction. *ACS Appl. Nano Mater.* 2018, *1*, 5035−5043.

(49) Su, G.; Liu, L.; Liu, X.; Zhang, L.; Xue, J.; Tang, A. Magnetic Fe3O4@SiO2@BiFeO3/rGO composite for the enhanced visible-light catalytic degradation activity of organic pollutants. *Ceram. Int.* **2021**, *47*, 5374−5387.

(50) Borah, B. J.; Bharali, P. Direct Hydrogenation of Nitroaromatics at Room Temperature Catalyzed by Magnetically Recoverable Cu@ Fe2O3 Nanoparticles. *Appl. Organomet. Chem.* **2020**, *34*, No. e5753.

(51) Halligudra, G.; Paramesh, C. C.; Mudike, R.; Ningegowda, M.; Rangappa, D.; Shivaramu, P. D. PdII on Guanidine-Functionalized Fe3O4 Nanoparticles as an Efficient Heterogeneous Catalyst for Suzuki−Miyaura Cross-Coupling and Reduction of Nitroarenes in Aqueous Media. *ACS Omega* **2021**, *6*, 34416−34428.

(52) Yang, F.; Feng, A.; Wang, C.; Dong, S.; Chi, C.; Jia, X.; Zhang, L.; Li, Y. Graphene oxide/carbon nanotubes−Fe3O4 supported Pd nanoparticles for hydrogenation of nitroarenes and C−H activation. *RSC Adv.* **2016**, *6*, 16911−16916.

(53) Das, V. K.; Mazhar, S.; Gregor, L.; Stein, B. D.; Morgan, D. G.; Maciulis, N. A.; Pink, M.; Losovyj, Y.; Bronstein, L. M. Graphene Derivative in Magnetically Recoverable Catalyst Determines Catalytic Properties in Transfer Hydrogenation of Nitroarenes to Anilines with 2-Propanol. *ACS Appl. Mater. Int.* **2018**, *10*, 21356−21364.

(54) Zhou, P.; Li, D.; Jin, S.; Chen, S.; Zhang, Z. Catalytic transfer hydrogenation of nitro compounds into amines over magnetic graphene oxide supported Pd nanoparticles. *Int. J. Hydrogen Energy* **2016**, *41*, 15218−15224.

(55) Qiao, J.; Wang, T.; Zheng, K.; Zhou, E.; Shen, C.; Jia, A.; Zhang, Q. Magnetically reusable fe3o4@nc@pt catalyst for selective reduction of nitroarenes. *Catalysts* **2021**, *11*, 1219.

(56) Azadi, S.; Sardarian, A. R.; Esmaeilpour, M. Magnetically-recoverable Schiff base complex of Pd(II) immobilized on Fe3O4@ SiO2 nanoparticles: an efficient catalyst for the reduction of aromatic nitro compounds to aniline derivatives. *Monatsh. Chem.* **2021**, *152*, 809−821.

(57) Shokri, Z.; Zeynizadeh, B.; Hosseini, S. A.; Azizi, B. Magnetically nano core−shell Fe3O4@Cu(OH)x: a highly efficient and reusable catalyst for rapid and green reduction of nitro compounds. *J. Iran. Chem. Soc.* **2017**, *14*, 101−109.

(58) Mei, N.; Liu, B. Pd nanoparticles supported on Fe3O4@C: An effective heterogeneous catalyst for the transfer hydrogenation of nitro compounds into amines. *Int. J. Hydrogen Energy* **2016**, *41*, 17960−17966.